

## RESEARCH ARTICLE

10.1002/2014JA019988

## Key Points:

- Simultaneous observation of solar wind and terrestrial far tail by STEREO
- Terrestrial tail dynamics triggered by corotating interaction region passages
- Accelerated ions observed up to  $\sim 800 R_E$  distance from the Earth

## Correspondence to:

A. Opitz,  
aopitz@cosmos.esa.int

## Citation:

Opitz, A., et al. (2014), Solar wind control of the terrestrial magnetotail as seen by STEREO, *J. Geophys. Res. Space Physics*, 119, 6342–6355, doi:10.1002/2014JA019988.

Received 17 MAR 2014

Accepted 17 JUL 2014

Accepted article online 23 JUL 2014

Published online 20 AUG 2014

## Solar wind control of the terrestrial magnetotail as seen by STEREO

Andrea Opitz<sup>1,2</sup>, Jean-Andre Sauvaud<sup>2</sup>, Andreas Klassen<sup>3</sup>, Raul Gomez-Herrero<sup>4</sup>, Radoslav Bucik<sup>5</sup>, Lynn M. Kistler<sup>6</sup>, Christian Jacquey<sup>2</sup>, Janet Luhmann<sup>7</sup>, Glenn Mason<sup>8</sup>, Primoz Kajdic<sup>1,2</sup>, and Benoit Lavraud<sup>2</sup>
<sup>1</sup>ESTEC, European Space Agency, Noordwijk, Netherlands, <sup>2</sup>IRAP (CNRS-UPS), University of Toulouse, Toulouse, France,

<sup>3</sup>Institute of Experimental and Applied Physics, University of Kiel, Kiel, Germany, <sup>4</sup>Space Research Group, University of Alcalá, Alcalá de Henares, Spain, <sup>5</sup>Max-Planck-Institut für Sonnensystemforschung, Göttingen, Germany, <sup>6</sup>EOS, University of New Hampshire, Durham, New Hampshire, USA, <sup>7</sup>SSL, University of California, Berkeley, California, USA, <sup>8</sup>Johns Hopkins University Applied Physics Laboratory, Laurel, Maryland, USA

**Abstract** At the beginning of 2007 the twin STEREO spacecraft provided a unique opportunity to study the global solar wind control of the terrestrial magnetotail under typical solar activity minimum conditions. The STEREO-B (STB) spacecraft flew in the vicinity of the far terrestrial magnetotail, while the STEREO-A (STA) spacecraft was located in front of the Earth performing measurements in the undisturbed solar wind. In February, the STB spacecraft was located in the magnetosheath most of the time but experienced several incursions into the distant magnetotail. Comparison of STA and STB observations determines unambiguously whether solar wind events such as energetic particle enhancements observed by STB are of pure solar origin or due to the influence of the terrestrial magnetosphere. During this time period in 2007, there were solar minimum conditions with alternating fast and slow solar wind streams that formed corotating interaction regions, which were the dominating source of magnetospheric disturbances encountering the Earth almost every week. Under these conditions, STB experienced multiple bow shock and magnetopause crossings due to the induced highly dynamic behavior of the terrestrial magnetotail and detected bursts of tailward directed energetic ions in the range of 110–2200 keV accompanied by suprathermal electrons of  $\sim 700$ –1500 eV, which were not seen in the undisturbed solar wind by STA. The corotating interaction regions triggered these energetic particle enhancements, and we demonstrate their magnetosphere-related origin. Even after leaving the magnetosheath in March 2007, STB continued to observe antisunward directed energetic ion bursts until May up to a distance of  $\sim 800 R_E$  behind Earth, the largest distance to which solar wind and magnetospheric interaction has been observed. These results show that Earth is a very significant source of energetic particles in its local interplanetary environment.

## 1. Introduction

At the beginning of 2007 the twin Solar Terrestrial Relations Observatory (STEREO) mission [Kaiser et al., 2008] provided a unique opportunity to perform observations simultaneously in the far tail of the terrestrial magnetosphere and in the undisturbed solar wind. Figure 1 gives the location of the spacecraft in the X-Y GSM plane. The STEREO Ahead (STA) spacecraft was in front of the Earth, while the STEREO Behind (STB) spacecraft flew in the vicinity of the terrestrial magnetotail and crossed different plasma regions there. In February the STB spacecraft was located in the dusk magnetosheath most of the time but experienced several incursions into the distant magnetotail [Kistler et al., 2010; Sauvaud et al., 2011]. Then in March, STB finally left the terrestrial magnetosheath and flew into the solar wind.

In the present paper we compare STA observations of pure solar wind with measurements taken simultaneously on board the STB, which are perturbed by the Earth's magnetosphere. The simultaneous STA and STB observations of the distant magnetotail are unique since their instrumentation is nearly identical, so their measurements are easily comparable. Before May 2007 the spacecraft heliocentric longitudinal separation was relatively small ( $< 10^\circ$ ). On such spatial scales, the bulk solar wind properties are generally persistent [Opitz et al., 2009, 2010]; thus, comparisons of solar wind properties measured by the two STEREO spacecraft results in a very good correlation. Hence, we can assume that any significant differences between STA and STB observations are most probably due to the terrestrial magnetospheric plasma regimes sensed by STB.

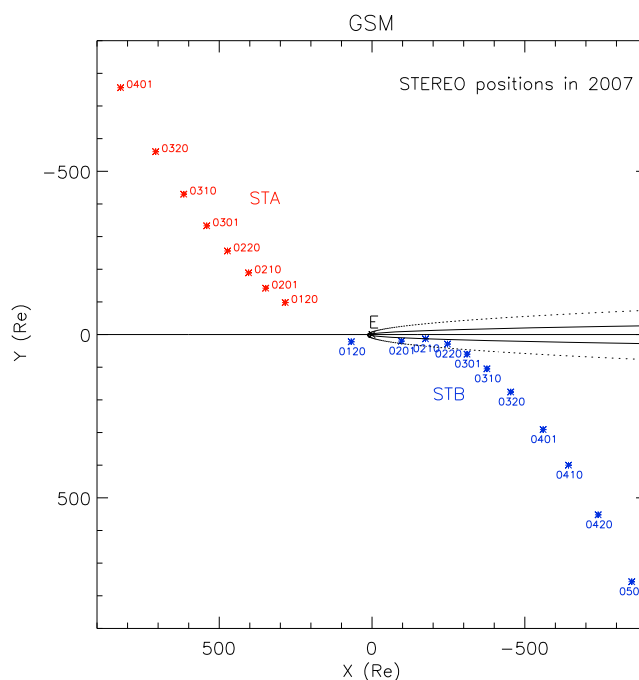


**Figure 1.** Positions of the STA (red) and STB (blue) spacecraft from January to May 2007. Numbers denote month and day in the format MMDD. The bow shock and magnetopause are drawn around the Earth just approximately; they were both very dynamic during the investigated period.

Although the STEREO spacecraft are designed for solar and heliospheric observations, we can derive limited but original magnetospheric information from the comparison of their plasma and magnetic field measurements. We will in particular show that energetic particles accelerated inside the magnetosphere and at its boundaries populate the distant magnetosheath and can even be detected in the solar wind at a distance of  $\sim 800 R_E$  from the Earth.

Previous observations of the terrestrial far tail were performed in detail by the Geotail mission in the 1990s up to a distance of  $\sim 200 R_E$ , where the IMP 8 and Wind spacecraft were used as a solar wind monitor in order to explain the phenomena observed in the magnetotail [Nishida *et al.*, 1997, and references therein]. Tailward ion flow of  $< 200$  keV was reported in the distant magnetosphere ( $\sim 200 R_E$ ), more precisely inside the plasma sheet by Christon *et al.* [1996]. Far

beyond these Geotail observations, STEREO observed ion bursts in the magnetosheath and the solar wind behind Earth up to a distance of  $800 R_E$ .

There are four main sources of energetic ion increases observed in the solar wind near the Earth: solar energetic particle (SEP) events, corotating interaction regions (CIRs), bow shock acceleration, and particle leakage from the terrestrial magnetosphere. SEP events associated with solar activity phenomena such as flares and coronal mass ejections (CMEs) are dominant near solar maximum. During solar quiet time periods, CIRs are a well-known source of energetic ions with energies up to a few MeV per nucleon [e.g., McDonald *et al.*, 1976; for a complete review on CIRs and energetic particles see Richardson, 2004]. The early phase of the STEREO mission (2007–2009), which coincides with a quiet solar minimum, thus provides a unique opportunity for multipoint studies of CIR-associated ion increases [e.g., Gomez-Herrero *et al.*, 2009, 2011; Dresing *et al.*, 2009; Mason *et al.*, 2009; Bucik *et al.*, 2012].

After the STEREO launch, these quiet conditions were also favorable for the study of energetic ions originating from the Earth's magnetosphere or from the bow shock. Short-duration energetic ion events originating from the Earth are frequently observed in the upstream region of the Earth's bow shock. These events, commonly named "magnetospheric" or "upstream" events, are characterized by energetic ion fluxes streaming from the Earth's direction toward the Sun, with energies below 1 MeV. They were detected very often during the near-Earth phase of the STEREO orbit, especially during disturbed magnetosphere intervals, for instance during the arrival of high-speed solar wind streams [Müller-Mellin *et al.*, 2008b; Desai *et al.*, 2008; Klassen *et al.*, 2009; Kronberg *et al.*, 2011]. Upstream ion events are occasionally coincident with energetic electron increases (energies below 300 keV), and they have been explained either as leakage of magnetospheric particles accelerated within the magnetosphere [e.g., Sarris *et al.*, 1978; Krimigis *et al.*, 1978] or as acceleration at the bow shock itself [e.g., Scholer *et al.*, 1981; Burgess, 2007, and references therein]. Furthermore, Klassen *et al.* [2009] reported the detection of a special kind of energetic particle event by STEREO close to Earth's bow shock, the so-called almost monoenergetic ion (AMI) events, showing an energy spectrum containing one or more narrow peaks with a relative full width half at maximum of 0.1–0.7 [see also Lutsenko and Kudela, 1999], in contrast with the typical upstream events showing a power law energy distribution. Similar AMI events were observed far away from the Earth, so they seem to be also present during passages of interplanetary shocks [Klassen *et al.*, 2011].

## 2. STEREO Data

The In situ Measurements of Particles and CME Transients (IMPACT) investigation [Luhmann *et al.*, 2008] on board the STEREO mission provides multipoint solar wind electron, interplanetary magnetic field, and solar energetic particle measurements. As part of this complex instrument package the Solar Electron Proton Telescope (SEPT) measures energetic particles: electrons in the energy range of 30–400 keV and ions with energies of 60–7000 keV [Müller-Mellin *et al.*, 2008a]. SEPT consists of four 52° conical apertures looking in four different directions: two in the ecliptic plane along the Parker spiral, sunward (upstream, SEPT-U) and antisunward (downstream, SEPT-D), as well as two oriented perpendicular to the ecliptic plane, northward (SEPT-N) and southward (SEPT-S). The Solar Wind Electron Analyzer (SWEA) top hat experiment [Sauvaud *et al.*, 2008] provides in situ electron measurements at both STEREO spacecraft in the energy range of 1–2000 eV. The SWEA in-flight calibration results were reported by Fedorov *et al.* [2011], and the electron density data are from the data set created by Opitz *et al.* [2010]. The in situ magnetic field measurements are provided by the magnetometer (MAG) experiment [Acuna *et al.*, 2008] on board the twin spacecraft. In our study we also make use of energetic heavy-ion observations obtained by the Suprathermal Ion Telescope (SIT) experiment on STEREO [Mason *et al.*, 2008a]. The SIT instrument is a time-of-flight mass spectrometer which measures ions from helium to iron in the energy range of 20 keV/n to a few MeV/n.

The Plasma and Suprathermal Ion Composition (PLASTIC) experiment [Galvin *et al.*, 2008] on board the STEREO measures solar wind ions in situ in the energy range of 0.2–86 keV. It is a hemispherical electrostatic analyzer (selection of energy-per-charge) with a solar wind sector, whose aperture is pointing always toward the Sun with a field of view of  $\pm 22.5^\circ \times \pm 20^\circ$  (in- and out-of-ecliptic angles, respectively). It has a novel ion optical design that uses two different solar wind apertures, one for less abundant and one for more abundant solar wind elements. Lower ion fluxes are measured by the Main channel (MC), while higher ion fluxes are measured by the S-shaped channel (SC), which has a much smaller geometric factor. If the count rate measured through the Main channel exceeds a commandable value during the high-to-low energy sweep, an electronic switch changes to the S-channel, which reduces the count rate to an acceptable value. The switch is usually triggered around the helium peak.

## 3. CIR Control of the Terrestrial Plasma Environment

In the first half of 2007, there was only one major geoeffective CME (end of May in Figure 2) observed by the two STEREO spacecraft, and rather, CIRs were the dominant geoeffective solar disturbances. STEREO mainly observed alternating fast and slow solar wind streams in 2007. Figure 2 shows in situ data from STA for the time period 1 February to 1 June 2007. Figure 2 (first panel) shows the PLASTIC solar wind proton bulk velocity. Where the fast solar wind plasma tries to overtake the preceding slow solar wind, the streams interact and form a compression region characterized by density enhancement (Figure 2, second panel), magnetic field enhancement (Figure 2, third panel), and magnetic field variation. These stream interaction regions (SIRs) are often recurrent during solar minimum hence termed corotating interaction regions (CIRs) by Pizzo [1978].

The CIRs enhanced by grey shading in Figure 2 are accompanied by energetic ion increases (fourth panel), which are seen in all SEPT look directions. On the other hand, there are CIRs that do not come with energetic ion enhancements, though they can still be similarly geoeffective. As an example, Figure 3 compares the STA and STB data with the auroral electrojet (AE) index during such a CIR event. Note that this time both STEREO spacecraft were outside the terrestrial magnetosphere. Upon the CIR arrival, the increase in the plasma pressure and the varying magnetic field direction with its enhanced magnitude (third and fifth panels) are responsible for terrestrial magnetic activity, which is quantified here by the AE index (fourth panel). The geoeffectiveness of the solar disturbance depends on the interplanetary magnetic field (IMF) orientation since the solar energy transfer from the solar wind to the magnetosphere is more efficient during southward IMF (large-scale reconnection). As a result, a good correlation between negative  $B_z$  and the AE index [Akasofu, 1981; Perreault and Akasofu, 1978; Russell and McPherron, 1973] can be easily seen in Figure 3. The solar wind control of the terrestrial space weather is clear; the magnetic activity of the Earth is strongly enhanced during and after the CIR arrival.

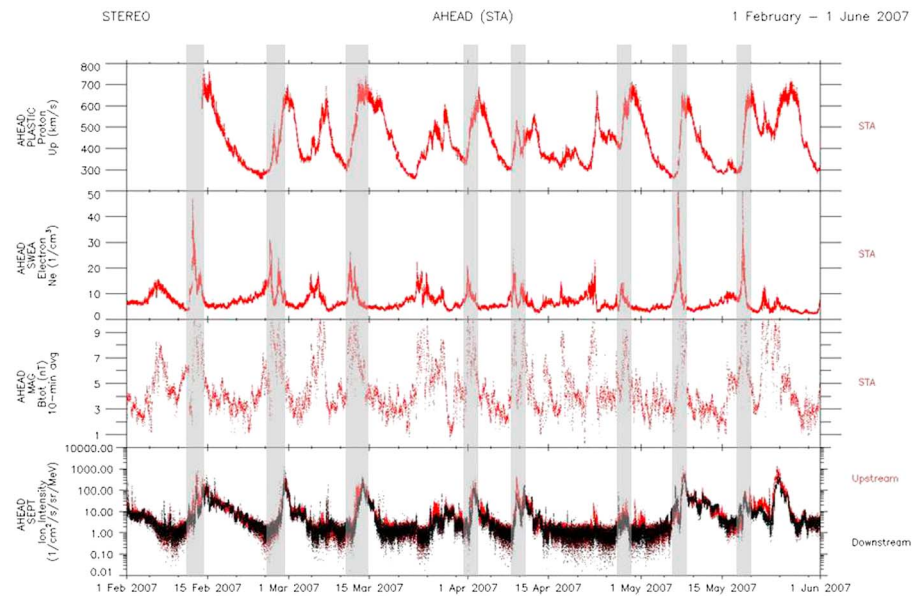
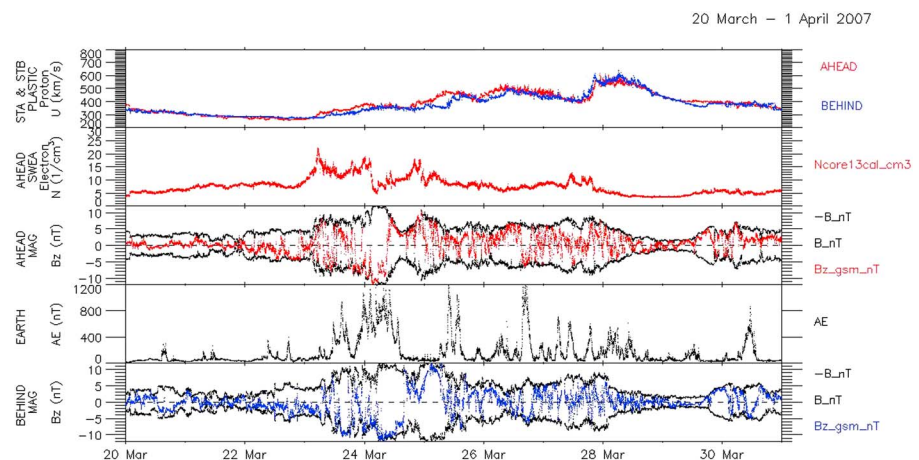


**Figure 2.** STEREO Ahead measurements from 1 February 2007 to 1 June 2007. (first panel) PLASTIC bulk velocity. (second panel) SWEA electron density proxy. (third panel) MAG magnetic field magnitude ( $B_{\text{tot}}$ ). (fourth panel) SEPT ion intensity between 110 keV and 2200 keV (black: downstream look direction / sunward particles, red: upstream look direction / antisunward particles). Grey-shaded regions mark the time intervals of well-developed CIRs with clear energetic ion enhancement.

#### 4. Magnetospheric Regimes Crossed by STB

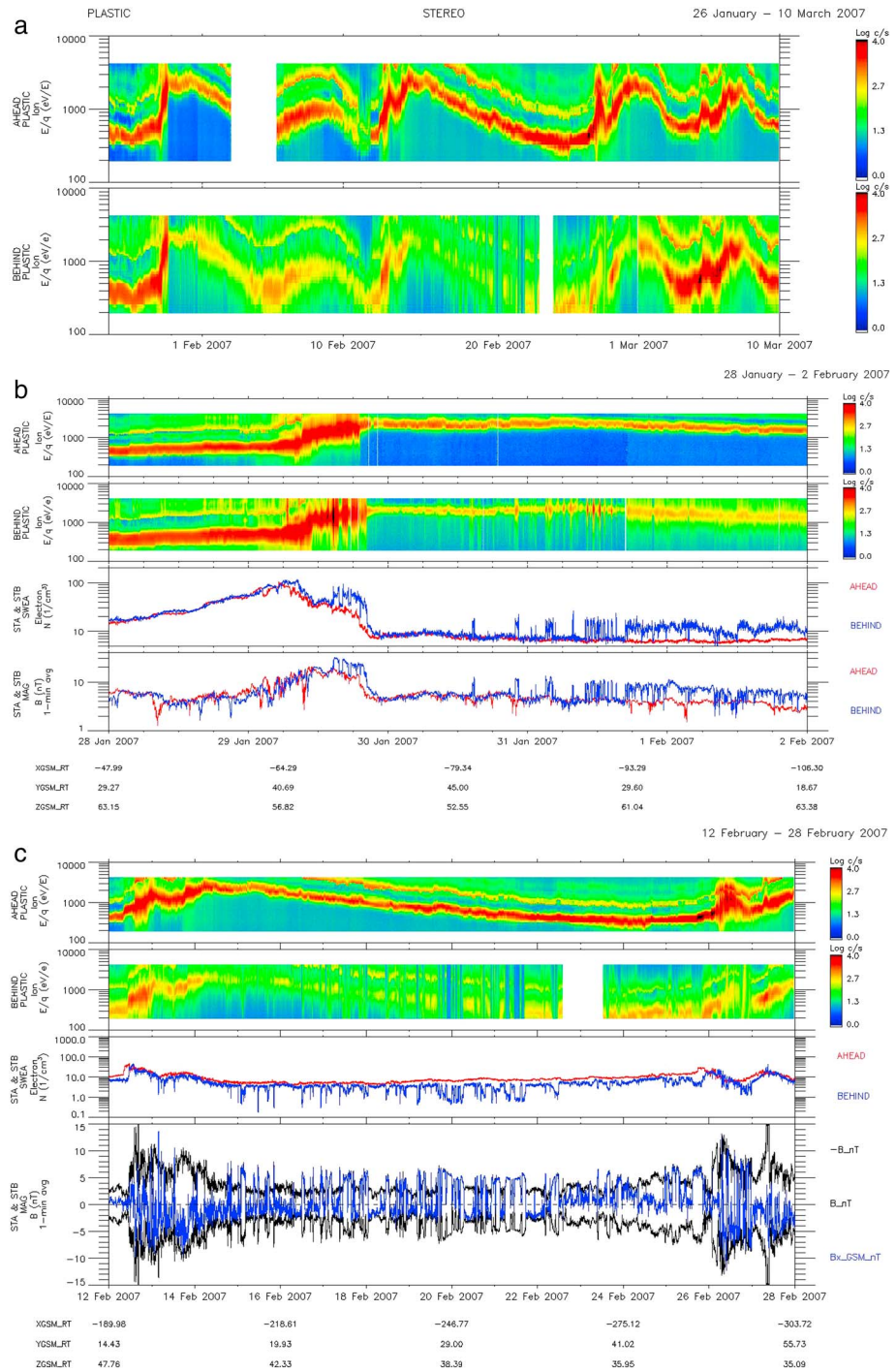
During our STEREO observation of the terrestrial plasma environment in 2007 we find that the magnetotail becomes very dynamic after the CIR passages. The STB spacecraft crosses through different plasma regimes while moving along the duskside magnetotail. The differences between STA and STB PLASTIC ion and MAG magnetic field measurements in Figure 4 are thus due to the fact that the two spacecraft are located in different plasma regions. While the STA spacecraft is located in the upstream solar wind, the STB spacecraft is usually located in the terrestrial magnetosheath with several incursions into the distant magnetotail.

Figure 4a shows the PLASTIC low-energy ion energy-time spectrograms recorded from 26 January to 10 March 2007 by STA (top) and STB (bottom). Protons ( $H^+$ ) are the most abundant ions in the plot; their



**Figure 3.** STEREO measurements from 20 March to 31 March 2007. (first panel) STA and STB PLASTIC bulk velocity. (second panel) STA SWEA electron core density proxy. (third and fifth panels) STA and STB MAG magnetic field magnitude ( $B_{\text{tot}}$  and  $-B_{\text{tot}}$ ) and z component in GSM coordinate system ( $B_z$ ). (fourth panel) AE index (World Data Center for Geomagnetism in Kyoto).





**Figure 4.** (a) STA (top) and STB (bottom) PLASTIC energy spectrograms on 26 January to 10 March 2007. Note that on the PLASTIC energy spectra helium is clearly visible above the proton peak since the instrument switches from a larger (MC) to a smaller (SC) aperture during the high-to-low energy sweep when the count rate reaches a certain limit, which falls usually on the helium peak in the solar wind. (b) STA and STB PLASTIC energy spectrograms, SWEA electron density, and 1-minute averaged MAG magnetic field measurements during multiple bow shock crossings on 28 January to 2 February 2007. (c) STA and STB PLASTIC energy spectrograms, SWEA electron density, and 1-minute averaged MAG magnetic field measurements during multiple magnetopause crossings on 12–28 February 2007.

energy varies around 1 keV. The second band is the  $\text{He}^{2+}$ , but note that it is distorted because the instrument switch between the two different solar wind apertures (MC and SC) falls on the helium peak.

In order to show the multiple bow shock crossings, Figure 4b zooms on the time period from 28 January to 2 February 2007. From top to bottom, the ion energy-time spectrograms, the SWEA solar wind core electron density, and the MAG magnetic field measurements are plotted. The STA (red) and the STB (blue) measurements are overplotted in order to show the different plasma regimes observed by the two spacecraft. They observe almost the same plasma properties as long as both spacecraft are in the solar wind. When STB crosses the terrestrial bow shock, the STB plasma density and the magnetic field jump while the STA observations remain nominal. On 29 January, there was a CIR arrival during the STB approach to the terrestrial bow shock. Due to the solar wind triggered dynamics of the terrestrial magnetosphere and due to the fact that the STB spacecraft crossed the bow shock at the flank, we observed multiple bow shock crossings, which are listed in Table 1. The transitions of STB into the magnetosheath can be identified by the enhanced density and magnetic field relative to the STA observations. Around 14:30 UT on 29 January, the STB spacecraft crossed the terrestrial bow shock for the first time at  $X_{\text{GSM}} = \sim -69 R_E$  and then entered and exited the magnetosheath sporadically until 03:44 UT on 1 February ( $X_{\text{GSM}} = \sim -98 R_E$ ), when it flew deeply into the magnetosheath.

In order to show the multiple magnetopause crossings, Figure 4c enlarges the time period from 12 to 28 February 2007. After the arrival of another CIR on 12 February, the STB spacecraft experienced several magnetotail incursions. These can be identified by the drops in the plasma density and the enhancements of the geotail field, which is much higher than in the solar wind, and it is dominantly aligned along the x direction (GSM). As the STB spacecraft flew through the structured far tail, the magnetotail moved back and forth, and the spacecraft exited and reentered the tail several times. The STB measurements show spatial variations due to the structured far tail along with temporal variations due to intensive tail dynamics leading to tail flappings, expansions, and contractions, which makes the observing spacecraft exit and enter the different plasma regimes. These multiple magnetopause crossings were studied by Kistler *et al.* [2010], who analyzed a plasma sheet crossing on 13 February 2007 and by Sauvaud *et al.* [2011], who studied three successive events on 21 February 2007, when STB exited the magnetotail due to tail contraction.

At the beginning of March 2007 the STB spacecraft apparently left the far terrestrial magnetosheath and observed pure solar wind conditions similar to STA. Though, as we will see later, these measurements still show energetic particle injections from the direction of the terrestrial magnetosphere.

## 5. Energetic Ions Ejected From the Terrestrial Magnetosphere Into the Magnetosheath and Into the Solar Wind

The relationship between the solar wind velocity, the energetic particles observed, and the AE index is shown in Figure 5a. In the time period studied here (February–June 2007), the STA spacecraft located in the upstream region of the terrestrial bow shock observed energetic particles from CIRs and upstream events. The purely CIR-related energetic ion enhancements are seen by all SEPT telescopes; the flux from 110 to 2200 keV in the sunward (upstream) and antisunward (downstream) directions is shown in the second panel. At the same time, the STB spacecraft was behind the Earth and crossed the different regimes of the terrestrial plasma environment. STB observed the energetic ion enhancements from the CIRs, but additionally, it detected highly anisotropic energetic ion bursts coming from the Earth's direction (fourth panel). On STB, the ion flux coming from the Sun/Earth (upstream) direction is most of the time larger than the flux toward the Sun (downstream). In Figures 5b and 5c we show two observation periods in more detail: Figure 5b shows STB measurements in the magnetosheath (February–March 2007) and Figure 5c shows STB observations in the solar wind behind Earth (March–June 2007). The first and third panels again show the difference in anisotropy between the energetic particles observed on STA (top panel) with that observed on STB (third panel). The last four panels of Figures 5b and 5c show the SEPT ion spectrograms measured on board the STB. There are four look directions: northward, upstream, southward, and downstream. During the energetic ion burst events, the SEPT ion observations show the largest flux in the upstream look direction, a somewhat lower increase in the northward and southward directions, and the least increase in the downstream direction. This refers to a tailward or antisunward energetic ion flow.

**Table 1.** Bow Shock Crossing (BSC) Times in 2007 When STB Enters (in) and Exits (out) the Terrestrial Magnetosheath and the Corresponding Spacecraft Positions in Earth Radii ( $R_E$ ) and GSM Coordinates

Date		Time		Bow Shock Crossing (BSC)	STB Position		
Month	Day	Hour	Minute		X	Y	Z
January	29	14	30	in	−68.7	43.2	54.8
January	29	15	34	out	−69.2	40.7	56.6
January	29	16	8	in	−69.5	39.2	57.7
January	29	17	10	out	−70.0	36.3	59.5
January	29	17	34	in	−70.2	35.2	60.2
January	29	19	10	out	−71.0	30.7	62.5
January	29	19	18	in	−71.1	30.4	62.7
January	29	20	23	out	−71.6	27.8	63.8
January	30	14	29	in	−80.5	41.1	55.5
January	30	14	38	out	−80.6	40.8	55.7
January	30	14	46	in	−80.7	40.5	55.9
January	30	14	50	out	−80.7	40.4	56.0
January	30	21	50	in	−84.0	23.2	64.8
January	30	22	20	out	−84.3	22.7	64.9
January	30	22	23	in	−84.3	22.7	64.9
January	30	22	29	out	−84.3	22.6	64.9
January	31	3	3	in	−86.5	27.7	62.7
January	31	3	21	out	−86.6	28.5	62.4
January	31	3	30	in	−86.7	28.9	62.1
January	31	4	9	out	−87.0	30.8	61.2
January	31	4	12	in	−87.0	31.0	61.1
January	31	4	17	out	−87.0	31.2	61.0
January	31	7	39	in	−88.6	40.4	55.2
January	31	7	52	out	−88.7	40.8	54.8
January	31	9	53	in	−89.6	43.2	52.8
January	31	9	59	out	−89.7	43.3	52.8
January	31	10	7	in	−89.7	43.3	52.7
January	31	10	9	out	−89.7	43.4	52.7
January	31	10	12	in	−89.8	43.4	52.7
January	31	10	25	out	−89.9	43.4	52.6
January	31	10	42	in	−90.0	43.5	52.6
January	31	10	56	out	−90.1	43.4	52.6
January	31	11	5	in	−90.2	43.4	52.6
January	31	11	29	out	−90.3	43.2	52.7
January	31	11	31	in	−90.4	43.2	52.7
January	31	11	35	out	−90.4	43.2	52.8
January	31	11	48	in	−90.5	43.0	52.9
January	31	12	2	out	−90.6	42.9	53.0
January	31	12	6	in	−90.6	42.8	53.0
January	31	12	9	out	−90.7	42.7	53.1
January	31	12	16	in	−90.7	42.6	53.2
January	31	12	34	out	−90.8	42.3	53.4
January	31	12	48	in	−90.9	42.0	53.6
January	31	12	51	out	−91.0	42.0	53.7
January	31	13	2	in	−91.0	41.7	53.8
January	31	13	14	out	−91.1	41.4	54.1
January	31	13	47	in	−91.4	40.4	54.7
January	31	13	51	out	−91.4	40.3	54.8
January	31	14	23	in	−91.7	39.2	55.6
January	31	14	32	out	−91.7	38.9	55.8
January	31	15	8	in	−92.0	37.5	56.7
January	31	15	15	out	−92.1	37.2	56.9
January	31	16	45	in	−92.7	33.2	59.2
January	31	17	5	out	−92.9	32.2	59.7
January	31	17	7	in	−92.9	32.1	59.8
January	31	21	24	out	−94.8	21.7	64.1
January	31	21	42	in	−94.9	21.3	64.2
February	1	3	36	out	−97.5	27.1	61.6
February	1	3	44	in	−97.6	27.5	61.4

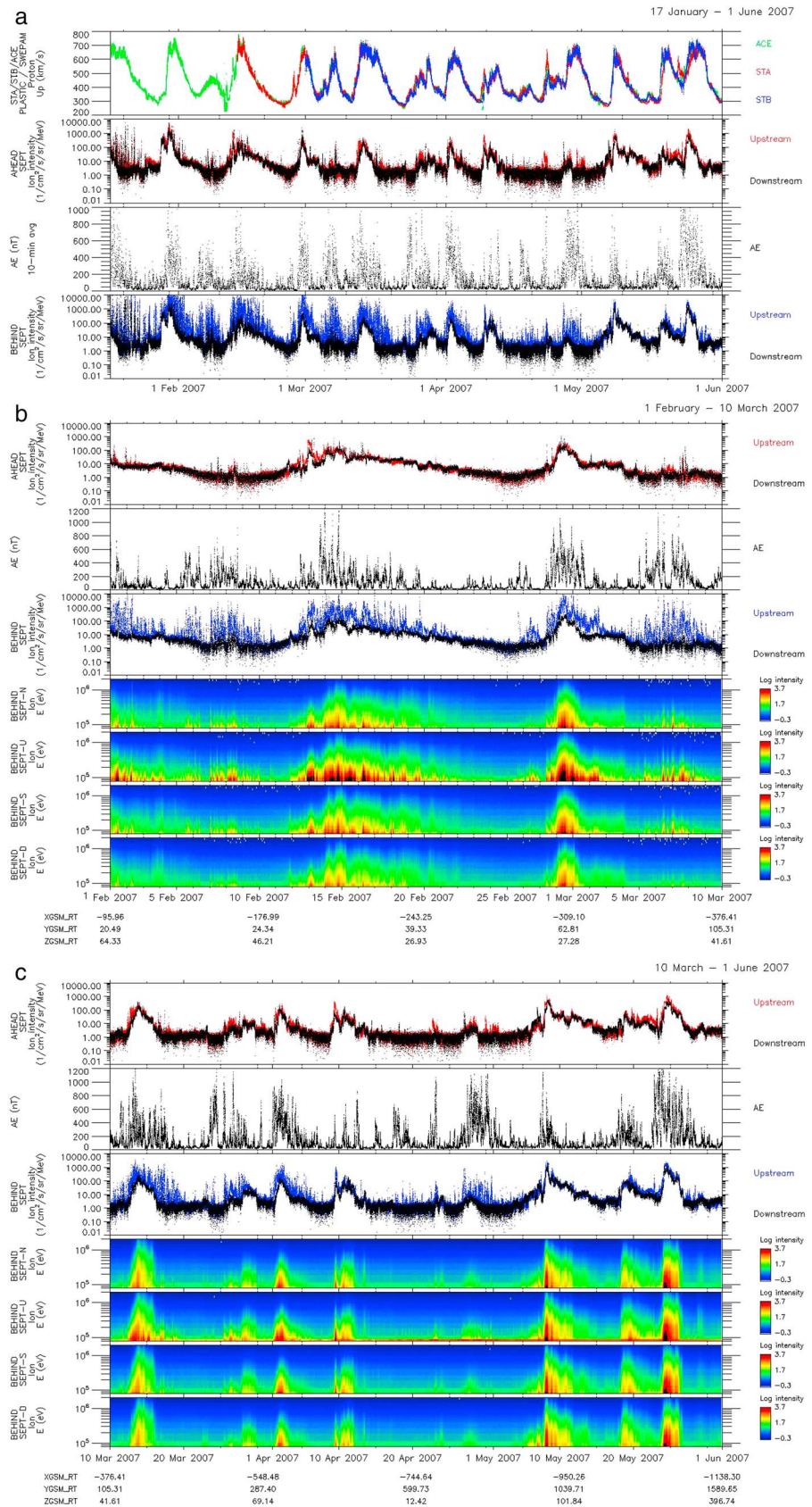
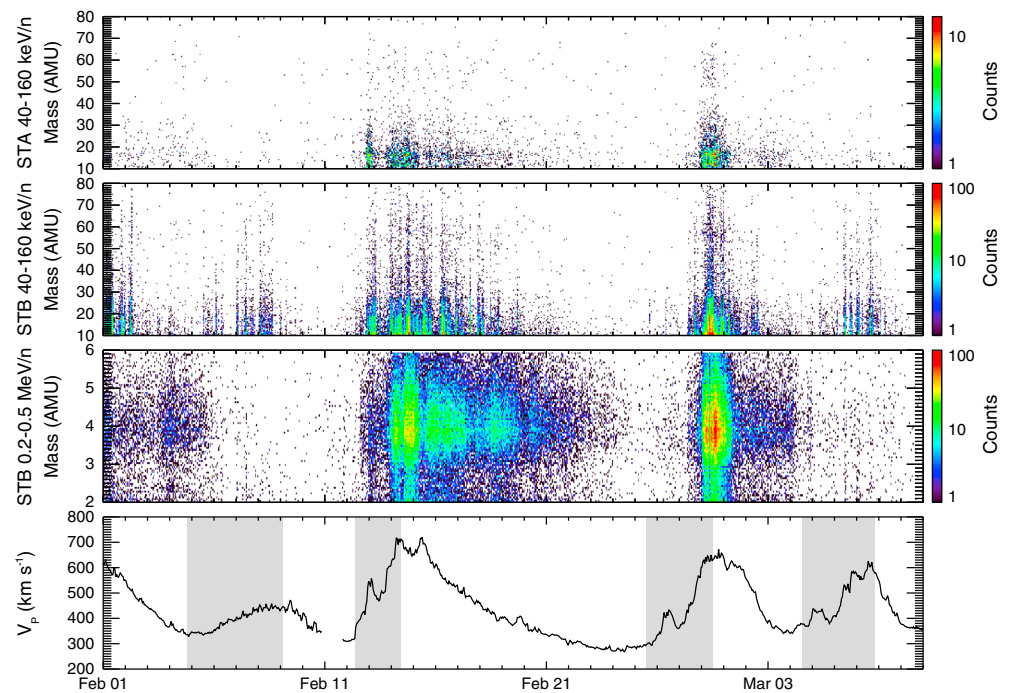


Figure 5





**Figure 6.** STEREO measurements from 1 February to 10 March 2007. (first and second panels) STEREO-A and STEREO-B heavy-ion SIT mass spectrograms at 40–160 keV/n. (third panel) STEREO-B helium mass spectrogram at 0.2–0.5 MeV/n. (fourth panel) 1-hour solar wind speed from SWEPAM on ACE. Shaded regions mark the time intervals of CIRs obtained from the ACE CIR list ([http://www-ssc.igpp.ucla.edu/~jlan/ACE/Level3/SIR\\_List\\_from\\_Lan\\_Jian.pdf](http://www-ssc.igpp.ucla.edu/~jlan/ACE/Level3/SIR_List_from_Lan_Jian.pdf)).

In all cases, a clear correlation between increases in fluxes in the upstream look direction and the *AE* index is observed, pointing to a magnetosphere-related origin.

All in all, it is clear that the energetic ion enhancements at CIRs have an additional increase through a tailward flow (as also observed by *Gomez-Herrero et al.* [2009]) when the observing spacecraft is in the proximity of the terrestrial magnetotail. Such events are multiple short-duration spikes on top of the enhanced background ion fluxes of CIR origin. This additional ion burst is well correlated with terrestrial magnetic activity (Figure 5a, third panel). It is present even after the spacecraft exits the magnetosheath, and it finally dies out by May 2007 (Figure 5a) when STB is farther than  $\sim 800 R_E$  from Earth (Figure 5c). It declines with distance from Earth since the probability of magnetic connectivity between the source and the spacecraft decreases. We note that despite the large distance ( $>1500 R_E$ ), there are a few spikes observed by the STB spacecraft end of May 2007 (Figure 5c) due to the geomagnetic storm caused by a CME.

Figure 6 shows SIT mass spectrograms from STA (first panel), STB (second and third panels), and solar wind speed (fourth panel) for the period from 1 February to 10 March 2007. Above  $\sim 100$  keV/nucleon, the

**Figure 5.** (a) STEREO measurements for the entire investigated time period from 17 January 2007 to 1 June 2007. ACE, STA, and STB proton bulk velocity (first panel). Ahead SEPT ion intensity between 110 keV and 2200 keV (black: downstream look direction / sunward particles, red: upstream look direction / antisunward particles) (second panel). *AE* index (World Data Center for Geomagnetism in Kyoto) (third panel). Behind SEPT ion intensity between 110 keV and 2200 keV (black: downstream look direction / sunward particles, blue: upstream look direction / antisunward particles) (fourth panel). (b) STEREO measurements zoomed on the magnetosheath period from 1 February to 10 March 2007. Ahead SEPT ion intensity between 110 keV and 2200 keV (black: downstream look direction / sunward particles, red: upstream look direction / antisunward particles) (first panel). *AE* index (World Data Center for Geomagnetism in Kyoto) (second panel). Behind SEPT ion intensity between 110 keV and 2200 keV (black: downstream look direction / sunward particles, blue: upstream look direction / antisunward particles) (third panel). Behind SEPT ion spectrograms in four look directions: northward, upstream, southward, and downstream, respectively (last four panels). The STB spacecraft coordinates are given in GSM coordinates. (c) STEREO measurements zoomed on the period of the disturbed solar wind behind Earth from 10 March to 1 June 2007. The panels show the same parameters as in Figure 5b. The STB spacecraft coordinates are given in GSM coordinates.

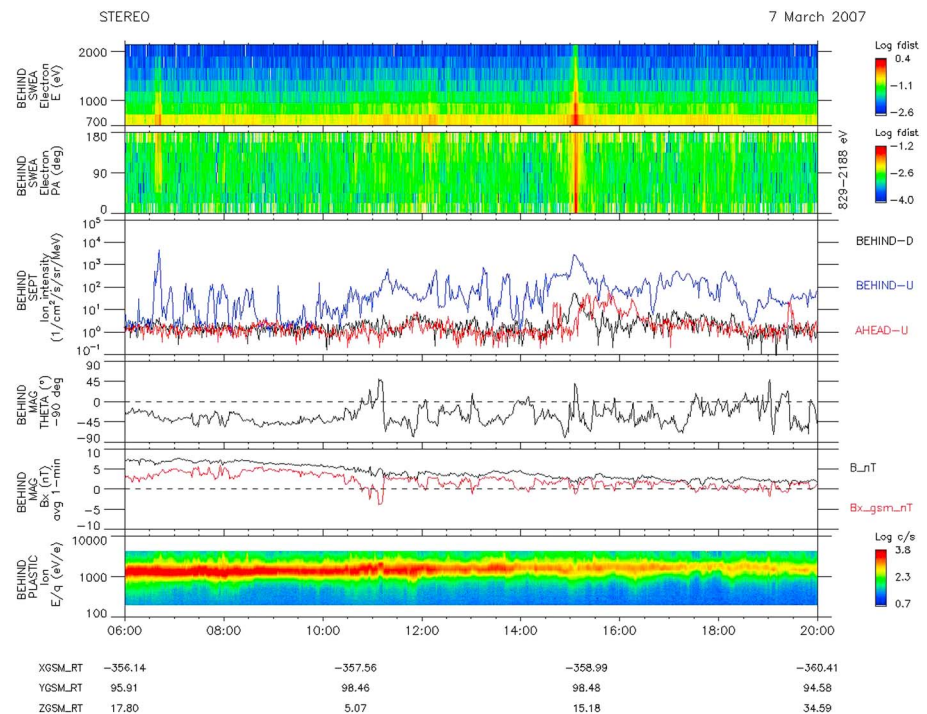


**Figure 7.** STEREO measurements on 7 March 2007. (first panel) Behind SWEA electron energy spectrogram. (second panel) Behind SWEA pitch angle distribution. (third panel) Behind (blue and black) and Ahead (red) SEPT ion intensities between 110 keV and 2200 keV by antisunward (D) and sunward (U) facing telescopes. (fourth panel) MAG magnetic field direction relative to  $X_{GSM}$  (90°: parallel, -90°: antiparallel). (fifth panel) MAG total magnetic field (black) and x component (red). (sixth panel) PLASTIC energy spectrogram.

composition of helium and heavier nuclei seen by STA and STB are both typical of CIR enhancements [e.g., *Mason et al.*, 2008b]. However, at lower energies, STB observed numerous brief, dispersionless increases (not shown) of ion intensities that have the same signatures as seen in “upstream events” observed from L1 [*Mason et al.*, 1996]. Particularly interesting are two periods with heavier-ion count enhancements observed by STB on 7–8 February and 6–7 March (second panel), but not on STA (first panel), which occurred during CIRs that encountered both spacecraft. These STB enhancements were observed near the C–O mass range and go up to Fe, making a magnetospheric origin unlikely. Note that near the C–O mass range individual peaks are not well resolved in SIT-B due to instrumental issues. Energetic helium (typical element enhanced in CIR events) was not observed in these two CIRs on both STB (see third panel) and STA (not shown) spacecraft. These two CIRs are examples of so-called “empty streams or CIRs,” quite often seen by STEREO and reported in previous studies [e.g., *Richardson et al.*, 1993]. The observations in Figure 6 suggest that heavier-ion enhancements seen on STB likely result from magnetosphere-related acceleration and their production or outflow was somehow triggered by the CIRs. The STB ions associated with CIRs on 12 and 25 February appear to be a mix of CIR and magnetosphere accelerated populations.

In a simple scenario, a short magnetic connectivity with the source of an energetic particle burst would be observed as a flux of ions and electrons with about the same velocity. In order to determine if this is observed, we searched for suprathermal electrons at energies corresponding to the velocity range of these antisunward flowing energetic ions by comparing electron bursts in the SWEA energy range with ion bursts in the SEPT energy range. Figure 7 shows an example in which a small subset of the tailward energetic ion bursts observed by STB was indeed accompanied by suprathermal electron enhancements. The SEPT antisunward energetic ion flow detected by STB at ~06:45 is accompanied by antiparallel (180° pitch angle) suprathermal electrons at a positive interplanetary magnetic field x component ( $B_x$ ) in the GSM coordinate system, which means that the suprathermal electrons flow also in the antisunward direction. The SEPT ion enhancement at 15:00 was detected by both STA and STB, but at STB it was superposed by antisunward energetic ion flow. This energetic ion enhancement is accompanied by suprathermal electrons at STB with

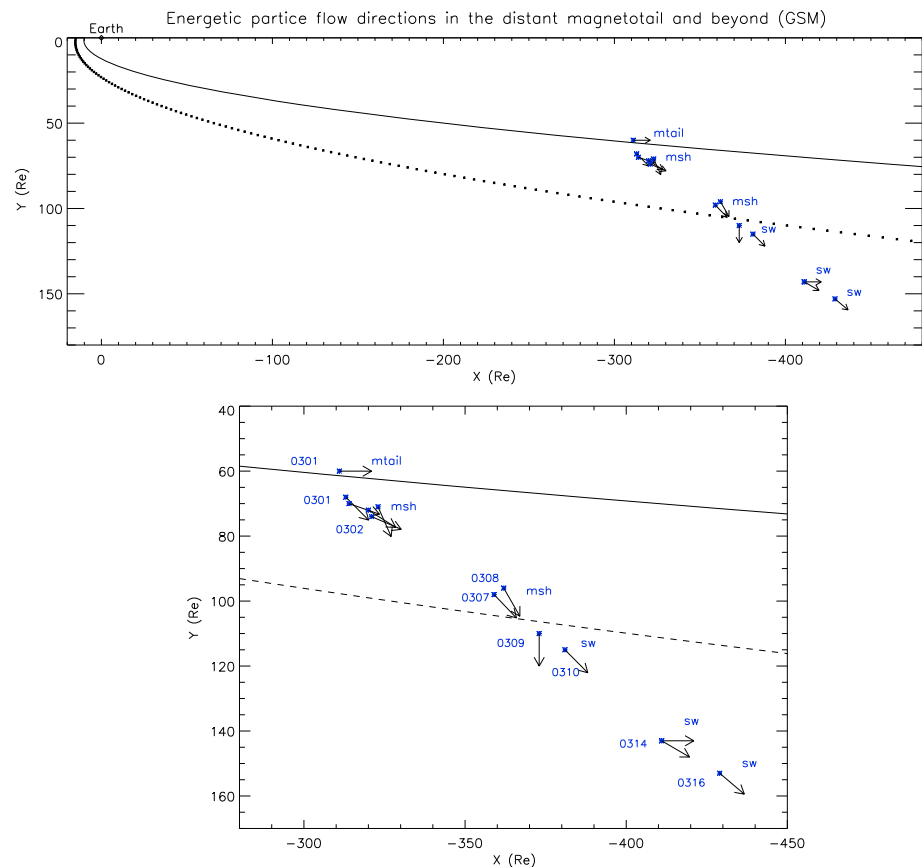


**Figure 8.** Energetic particle flow directions during simultaneous energetic ion and suprathermal electron peaks observed in the distant magnetotail and beyond by STB. The upper plot is to show how far from Earth these observations were, and the lower plot is a zoom. The bow shock and magnetopause are drawn around Earth just approximately; they were both very dynamic during the investigated period. The blue numbers denote month and day of the observation in the format MMDD, and the blue abbreviations stand for the plasma region where the STB spacecraft was located during the observation: mtail = magnetotail, msh = magnetosheath, and sw = solar wind.

isotropic pitch angle distribution (PAD). There is a clear agreement between energetic ions and suprathermal electrons: when the ions are anisotropic, the electrons are as well. The energy of the electrons is in the 700 eV to 1 keV range, while the energy of ions is 110 keV to 2200 keV. Note that a 1900 keV proton has the same velocity as a 1 keV electron, so the energy ranges of the observed proton and electron bursts are compatible with the fact that STB is connected to the source region for a short time.

It must be stressed that while STB exited the terrestrial magnetosheath in March 2007, it continued observing these magnetospheric events until May 2007 up to  $\sim 800 R_E$ , the largest distance to which solar wind and magnetospheric interaction has been observed.

## 6. Discussion

The energetic ion excess observed on STB is due to the proximity of the terrestrial magnetosphere since we find a decay with distance (Figure 5a, fourth panel) and a strong association with geomagnetic activity (Figures 5b and 5c). Additional proof is the flow direction; both the energetic ions and electrons come from the direction of the terrestrial magnetosphere. We do not see the same energetic particles on the STA spacecraft that is located in front of the Earth. The observation of these bursty energetic particle fluxes in the magnetosheath and the solar wind is possible when there is a magnetic connection between the observing spacecraft and the terrestrial magnetosphere or the Earth's bow shock. Note that, as exemplified in Figure 5b, the ion fluxes of magnetospheric origin can exceed by a factor 1000 the solar energetic particles fluxes.

As STB gets farther away from the Sun-Earth line ( $X_{\text{GSM}}$ ), we expect to find larger angular deviations between the magnetic field and the  $X_{\text{GSM}}$  direction during the events with simultaneous energetic ion and suprathermal electron peaks (such as shown in Figure 7). Figure 8 shows the presumed energetic particle flow direction derived from the magnetic field orientation during these events. Indeed, the flow direction tends to turn away from the Sun-Earth line as a function of increasing  $Y_{\text{GSM}}$  when STB is located inside the magnetosheath ( $Y_{\text{GSM}} < \sim 105 R_E$ ). This result shows, as expected, that the magnetosheath magnetic field lines bend toward the  $X_{\text{GSM}}$  direction with decreasing distance to this axis, which is consistent with flaring and probable connectivity of the whole magnetosheath with the magnetosphere. On the other hand, in the solar wind the magnetic configuration is not affected by the Earth and merely follows the IMF, though we can detect energetic particles. Gosling *et al.* [1987] showed that the IMF can connect to the magnetosphere and then loop around so that away looking instruments will see upstream event particles on these field lines.

This excess of ion flux is due to magnetospheric leakage or solar wind ions accelerated at magnetospheric discontinuities, or a combination of the two processes. In both cases, the energetic ion enhancement is triggered by the solar wind, either by activating the terrestrial magnetosphere or interacting with it. We conclude that the solar wind control of the terrestrial magnetosphere is extremely powerful and also significantly affects its surroundings. It can produce an excess of energetic ions in the outer boundaries of the magnetosphere and in the solar wind by a factor of thousand (in Figure 7 at  $\sim 06:45$ ), affecting the surrounding regions to at least  $800 R_E$ .

## 7. Conclusions

We have investigated the terrestrial far tail region observed during quiet solar conditions by the IMPACT and PLASTIC experiments on board the STB spacecraft, taking advantage of the location of the STA spacecraft with nearly identical instrumentation in the upstream solar wind. These measurements are unique as the two STEREO spacecraft observed simultaneously the upstream solar wind and the very distant terrestrial magnetotail. As expected, magnetospheric activity was driven by the enhanced solar wind magnetic field with high  $B_z$  component in the heliospheric regions compressed by the arrival of fast flows. During the analyzed period, STA observed a number of such CIR-related structures, recurring with a pseudo period of about one week.

The STB spacecraft crossed the terrestrial bow shock at its flank at  $X_{\text{GSM}} \sim 90 R_E$  just after a CIR passage. The bow shock was very dynamic due to its interaction with the CIR. It expanded so that STB entered the magnetosheath and then it deflated, so STB exited again to the upstream solar wind. Multiple crossings are similarly observed for the magnetopause. As a consequence of a follow-up CIR, the magnetopause flaps, making STB enter and exit the terrestrial magnetotail many times.

We found strongly enhanced tailward energetic ion fluxes in the distant magnetosheath and even beyond, in the solar wind, during substorms when STB appeared to be connected to the magnetosphere by the interplanetary magnetic field. These energetic ion bursts were triggered by the CIRs, and they were sometimes even accompanied by suprathermal electrons arriving from the same direction (source) with the same velocity. The short duration of the suprathermal events indicates an impulsive nature of the source, compatible with substorm-induced acceleration.

According to our present understanding, the solar surface magnetic topology (e.g., coronal holes) defines the structure and properties of the expanding solar wind. Further structuring during propagation is affected by the solar rotation and the magnetohydrodynamic laws. These dynamics forms SIRs or, when persistent, CIRs, which impact the magnetosphere, increasing the global magnetic activity at Earth. This chain of interactions leads to the observed energetic particle injections into the magnetosheath and even into the solar wind, well beyond the Earth to at least  $800 R_E$  as observed here. The energetic ion fluxes of magnetosphere-related origin can at times be 1000 times higher than solar fluxes. The magnetosphere thus appears as a powerful accelerator converting a part of the impinging electromagnetic energy into particle kinetic energy and launching these accelerated particles in the surrounding space, in the tailward direction.

These results highlight some of the phenomena occurring during this unique observation period by the twin STEREO spacecraft. Follow-on work will include a more detailed multipoint investigation of the magnetopause and bow shock fluctuations and a precise study of the energetic particle ejection process.



## Acknowledgments

The authors are grateful for the STEREO/IMPACT and PLASTIC and ACE/SWEPAM teams for their data sets. The AE indices are provided by the World Data Center for Geomagnetism in Kyoto. A great thanks to Emmanuel Penou for informatics support by CL program and Lorna Ellis for her help with PLASTIC data. Further acknowledgements for fruitful discussions go to Nicolas Andre, Iannis Dandouras, Philippe Escoubet, Sandrine Grimald, Kostiantyn Grygorov, Christian Mazelle, Jimmy Raeder, Christopher T. Russell, Mariella Tatrallyai, Matt Taylor, and Andrew Walsh. The STEREO/SEPT and SIT projects are supported under grants 50 OC 1302 and 50 OC 1301 by the German Bundesministerium für Wirtschaft through the Deutsches Zentrum für Luft- und Raumfahrt (DLR). Raul Gomez-Herrero acknowledges the financial support from the Spanish MINECO under projects AYA2011-29727-c02-01 and AYA2012-39810-c02-01. The STEREO/SIT work at the Applied Physics Laboratory/Johns Hopkins University was supported by NASA contract SA4889-26309 from the University of California (Berkeley). Andrea Opitz and Primož Kajdic are currently Research Fellows at ESA ESTEC. The authors acknowledge the two reviewers for their constructive comments.

Larry Kepko thanks the reviewers for their assistance in evaluating this paper.

## References

- Acuna, M. H., D. Curtis, J. L. Scheifele, C. T. Russell, P. Schroeder, A. Szabo, and J. G. Luhmann (2008), The STEREO/IMPACT magnetic field experiment, *Space Sci. Rev.*, **136**, 203–226.
- Akasofu, S.-I. (1981), Energy coupling between the solar wind and the magnetosphere, *Space Sci. Rev.*, **28**, 121–190.
- Bucik, R., U. Mall, A. Korth, and G. M. Mason (2012), Abundances of suprathermal heavy ions in CIRs during the minimum of solar cycle 23, *Sol. Phys.*, **281**, 411–422.
- Burgess, D. (2007), Particle acceleration at the Earth's bow-shock, *Lect. Notes Phys.*, **725**, 161–190.
- Christon, S. P., G. Gloeckler, D. J. Williams, R. W. McEntire, and A. T. Y. Lui (1996), The downtail distance variation of energetic ions in Earth's magnetotail region: Geotail measurements at  $X > -208R_E$ , *J. Geomagn. Geoelectr.*, **48**, 615–627.
- Desai, M. I., G. M. Mason, R. Müller-Mellin, A. Korth, U. Mall, J. R. Dwyer, and T. T. von Rosenvinge (2008), The spatial distribution of upstream ion events from the Earth's bow shock measured by ACE, Wind, and STEREO, *J. Geophys. Res.*, **113**, A08103, doi:10.1029/2007JA012909.
- Dresing, N., R. Gomez-Herrero, B. Heber, R. Müller-Mellin, R. Wimmer-Schweingruber, and A. Klassen (2009), Multi-spacecraft observations of CIR-associated ion increases during the Ulysses 2007 ecliptic crossing, *Sol. Phys.*, **256**, 409–425.
- Fedorov, A., A. Opitz, J.-A. Sauvaud, J. Luhmann, D. W. Curtis, and D. E. Larson (2011), The IMPACT Solar Wind Electron Analyzer (SWEA): Reconstruction of the SWEA transmission function by numerical simulation and data analysis, *Space Sci. Rev.*, **161**(1–4), 49–62.
- Galvin, A. B., et al. (2008), The Plasma and Suprathermal Ion Composition (PLASTIC) investigation on the STEREO observatories, *Space Sci. Rev.*, **136**, 437–486.
- Gomez-Herrero, R., A. Klassen, R. Müller-Mellin, B. Heber, R. Wimmer-Schweingruber, and S. Böttcher (2009), Recurrent CIR-accelerated ions observed by STEREO SEPT, *J. Geophys. Res.*, **114**, A05101, doi:10.1029/2008JA013755.
- Gomez-Herrero, R., O. Malandraki, N. Dresing, E. Kilpua, B. Heber, A. Klassen, R. Müller-Mellin, and R. F. Wimmer-Schweingruber (2011), Spatial and temporal variations of CIRs: Multi-point observations by STEREO, *J. Atmos. Sol.-Terr. Phys.*, **73**, 551–565.
- Gosling, J. T., D. N. Baker, S. J. Bame, W. C. Feldman, R. D. Zwickl, and E. J. Smith (1987), Bidirectional solar wind electron heat flux events, *J. Geophys. Res.*, **92**, 8519–8535, doi:10.1029/JA092iA08p08519.
- Kaiser, M. L., T. A. Kucera, J. M. Davila, O. C. Cyr St., M. Guhathakurta, and E. Christian (2008), The STEREO mission: An introduction, *Space Sci. Rev.*, **136**, 5–16.
- Kistler, L. M., et al. (2010), Escape of  $O^+$  through the distant tail plasma sheet, *Geophys. Res. Lett.*, **37**, L21101, doi:10.1029/2010GL045075.
- Klassen, A., R. Gomez-Herrero, R. Müller-Mellin, S. Böttcher, B. Heber, R. Wimmer-Schweingruber, and G. M. Mason (2009), STEREO/SEPT observations of upstream particle events: Almost monoenergetic ion beams, *Ann. Geophys.*, **27**, 2077–2085.
- Klassen, A., R. Gomez-Herrero, R. Müller-Mellin, B. Heber, R. Wimmer-Schweingruber, A. Opitz, and J.-A. Sauvaud (2011), The almost monoenergetic ion event on 19 October 2009: SEPT/STEREO observations, *Astron. Astrophys.*, **528**(A84), doi:10.1051/0004-6361/201014563.
- Krimigis, S. M., D. Venkatesan, J. C. Barichello, and E. T. Sarris (1978), Simultaneous measurements of energetic protons and electrons in the distant magnetosheath, magnetotail, and upstream in the solar wind, *Geophys. Res. Lett.*, **5**, 961–964, doi:10.1029/GL005i011p00961.
- Kronberg, E. A., R. Bucik, S. Haaland, B. Klecker, K. Keika, M. I. Desai, P. W. Daly, M. Yamauchi, R. Gomez-Herrero, and A. T. Y. Lui (2011), On the origin of the energetic ion events measured upstream of the Earth's bow shock by STEREO, *J. Geophys. Res.*, **116**, A02210, doi:10.1029/2010JA015561.
- Luhmann, J. G., et al. (2008), STEREO IMPACT investigation goals, measurements, and data products overview, *Space Sci. Rev.*, **136**, 117–184, doi:10.1007/s11214-007-9170-x.
- Lutsenko, V. N., and K. Kudela (1999), Almost monoenergetic ions near the Earth's magnetospheric boundaries, *Geophys. Res. Lett.*, **26**, 413–415, doi:10.1029/1999GL000002.
- Mason, G. M., J. E. Mazur, and T. T. von Rosenvinge (1996), Energetic heavy ions observed upstream of the Earth's bow shock by the STEP/IMPACT instrument on Wind, *Geophys. Res. Lett.*, **23**, 1231–1234, doi:10.1029/96GL01035.
- Mason, G. M., A. Korth, P. H. Walpole, M. I. Desai, T. T. von Rosenvinge, and S. A. Shuman (2008a), The Suprathermal Ion Telescope (SIT) for the IMPACT/SEP investigation, *Space Sci. Rev.*, **136**, 257–284, doi:10.1007/s11214-006-9087-9.
- Mason, G. M., R. A. Leske, M. I. Desai, C. M. S. Cohen, J. R. Dwyer, J. E. Mazur, R. A. Mewaldt, R. E. Gold, and S. M. Krimigis (2008b), Abundances and energy spectra of corotating interaction region heavy ions observed during Solar Cycle 23, *Astrophys. J.*, **678**, 1458, doi:10.1086/533524.
- Mason, G. M., M. I. Desai, U. Mall, A. Korth, R. Bucik, T. T. von Rosenvinge, and K. D. Simunac (2009), In situ observations of CIRs on STEREO, Wind, and ACE during 2007–2008, *Sol. Phys.*, **256**, 393–408.
- McDonald, F. B., B. J. Teegarden, J. H. Trainor, T. T. von Rosenvinge, and W. R. Webber (1976), The interplanetary acceleration of energetic nucleons, *Astrophys. J.*, **203**, L149–L154.
- Müller-Mellin, R., S. Böttcher, J. Falenski, E. Rode, L. Duvet, T. Sanderson, B. Butler, B. Johlander, and H. Smit (2008a), The Solar Electron and Proton Telescope for the STEREO mission, *Space Sci. Rev.*, **136**, 363–389.
- Müller-Mellin, R., R. Gomez-Herrero, S. Böttcher, A. Klassen, B. Heber, R. Wimmer-Schweingruber, L. Duvet, and T. R. Sanderson (2008b), Upstream events and recurrent CIR-accelerated particle events observed by STEREO/SEPT, in *Proceedings of the 30th International Cosmic Ray Conference*, vol. 1, edited by R. Caballero et al., pp. 371–374, Universidad Nacional Autónoma de México, Mérida, Mexico.
- Nishida, A., T. Yamamoto, and T. Mukai (1997), The GEOTAIL mission: Principal characteristics and scientific results, *Adv. Space Res.*, **20**(4/5), 539–548.
- Opitz, A., et al. (2009), Temporal evolution of the solar wind bulk velocity at solar minimum by correlating the STEREO A and B PLASTIC measurements, *Sol. Phys.*, **256**(1–2), 365–377, doi:10.1007/s11207-008-9304-7.
- Opitz, A., et al. (2010), Temporal evolution of the solar wind electron core density at solar minimum by correlating the SWEA measurements from STEREO A and B, *Sol. Phys.*, **266**(2), doi:10.1007/s11207-010-9613-5.
- Perreault, P., and S.-I. Akasofu (1978), A study of geomagnetic storms, *Geophys. J. R. Astron. Soc.*, **54**, 547–573.
- Pizzo, V. (1978), A three-dimensional model of corotating streams in the solar wind, 1. Theoretical foundations, *J. Geophys. Res.*, **83**(A12), 5563–5572, doi:10.1029/JA083iA12p05563.
- Richardson, I. G. (2004), Energetic particles and corotating interaction regions in the solar wind, *Space Sci. Rev.*, **111**, 267–376, doi:10.1023/B:SPAC.0000032689.52830.3.
- Richardson, I. G., L. M. Barbier, D. V. Reames, and T. T. von Rosenvinge (1993), Corotating MeV/amu ion enhancements at  $\leq 1$  AU from 1978 to 1986, *J. Geophys. Res.*, **98**, 13–32, doi:10.1029/92JA01837.
- Russell, C. T., and R. L. McPherron (1973), Semiannual variation of geomagnetic activity, *J. Geophys. Res.*, **78**(1), 92–108, doi:10.1029/JA078i001p00092.

- Sarris, E. T., S. M. Krimigis, C. O. Bostrom, and T. P. Armstrong (1978), Simultaneous multispacecraft observations of energetic proton bursts inside and outside the magnetosphere, *J. Geophys. Res.*, *83*(A9), 4289–4305, doi:10.1029/JA083iA09p04289.
- Sauvaud, J.-A., et al. (2008), The IMPACT Solar Wind Electron Analyzer (SWEA), *Space Sci. Rev.*, *136*(1–4), 227–239.
- Sauvaud, J. A., A. Opitz, L. Palin, B. Lavraud, C. Jacquety, L. Kistler, H. U. Frey, J. Luhmann, D. Larson, and C. T. Russell (2011), Far tail (255  $R_E$ ) fast response to very weak magnetic activity, *J. Geophys. Res.*, *116*, A03215, doi:10.1029/2010JA016077.
- Scholer, M., D. Hovestadt, F. M. Ipavich, and G. Gloeckler (1981), Upstream energetic ions and electrons: Bow shock-associated or magnetospheric origin?, *J. Geophys. Res.*, *86*, 9040–9046, doi:10.1029/JA086iA11p09040.